Chapter 3

Advanced Electro-Spark Deposition Process on Metallic Alloys

Petrică Vizureanu, Manuela-Cristina Perju, Dragoş-Cristian Achiței and Carmen Nejneru

Additional information is available at the end of the chapter

http://dx.doi.org/10.5772/intechopen.79450

Abstract

This chapter will study the material base-surface multilayer system for various types of depositions (increasing the wear resistance of Fe-C alloy parts) whose compatibility with the substrate provides high-quality parts. Thus, this system of layers can be applied on both the new and worn parts, being able to recondition and reintroduce in an intensive exploitation regime any parts with complex configuration operating in dynamic conditions. Deposited layers will be obtained using electro-spark deposition (ESD) process, which is a technology that uses electrical energy stored in a capacitor to initialize an electrical spark between the cathode and the anode. The high temperature generated by the electrical spark leads to partial melting of substrate and mixing of it with the material of the electrode. Between the two electric sparks, the amount of the molten metal solidifies to form the surface layer. The ESD is a very well used process for materials manufacturing in many industrial sectors.

Keywords: deposition, microstructure, hardness, mass transfer, spark

1. Introduction

Scientific aim of this chapter fits the theme of the widely known under the name of engineered surfaces and seeks to make contributions in what is defined as thin-layer deposition or by combined methods. It is known that in such cases systems are characterized by contradictory layer-substrate properties and system design requires operating limit. The method of analysis clearly relates the design of the system material base-surface multilayer so that it responds well to its functional role in the efficient use of materials and also affordable. The literature shows the diversity of the applicability domain of the electro-spark deposition process and

the variety of filler materials and basic materials used. There are also a multitude of purposes of use: in obtaining amorphous layers, in obtaining epitaxial layers, layers with special physical, chemical, and mechanical properties (corrosion resistance, wear resistance, fatigue resistance, and shock resistance) [1–4].

It is noted that the main reasons that cause system need to replace some parts in the industry are the destruction of surface layer by corrosion, wear, fatigue, and mechanical shock. The properties of metallic materials have been improved [5, 6], in order to increase the adhesion of deposits to the base material layer using the layer of composite material by means of electro-spark deposition process.

Currently, electro-spark deposition process is gaining more ground to thin film deposition with various metallic materials, which gives the surface characteristics of hardness and high wear resistance [7–16]. Most studies have focused on the analysis of the mechanical properties of the material base-surface multilayer system and mass transfer behavior to obtain required properties and to control as much as possible the thickness of the deposited layer. But there are unsolved issues that deserve the attention of a detailed study. Going to these relevant issues in industrial practice, research conducted in different countries, like Japan, China, [17–19], and Ireland [20] had highlighted a number of concern technologies knowledge and fundamental character and experimental studies leading to improve properties of surface layers obtained using the method with pulsed electrical discharges. The wear, fatigue, and corrosion phenomena are the most aggressive factors that lead to scrapping one part. From this, situation results the high importance for the physical-chemical research of the phenomenon that takes place into these superficial layers in connection with coating technologies [21, 22]. One of the methods to process the materials is electro-spark deposition method that can allow to coat complex shaped and reduced dimension parts by extracting material from the surface of the part or developing coating layers by applying the compact material electrodes or by introducing into working area of powders or mix of powders. It is necessary that the surface layers have a good adherence to the part and especially a good connection to the sublayer. In some surface areas, high hardness layers are formed. Most studies are focused on chemical, physical, and mechanical properties of deposited layer and on mass transfer behavior, to obtain the properties imposed and to control as much as possible the coating layer thickness.

Compared with laser ablation technology, CVD, PVD, etc., the ESD method is technologically much easier to execute and requires no vacuum chamber or additional devices. The deposition can be done both automatically and manually, allowing a wide range of surface adjustments and ease of correcting surface quality.

2. ESD process description

The technology can be defined as a micro-pulsed welding technique that allows deposition of one “electrode material” on a metallic sublayer; mass transport is made in high current intensity and in short time periods. ESD method implies heat and mass transfer phenomena. Basically, multiple phenomena involve such as heating to incandescence, melting, and eventually evaporating of the electrode material. There is a stream of electrons, ions, and neutral fast atoms in the electric field between the electrodes. Electric field is concentrated on a

microportion of the piece where metal melting bath forms. Microalloying between base material and electrode melt generates the formation of nitrides, carbides, carbonitrides, and plasma through air decomposition (nitrogen and active oxygen). All these phenomena and others successively describe the formation of the hardened superficial layer through deposition.

The process of electro-spark deposition on the material surfaces is based on the electro-erosion phenomenon and the polar transfer of the anode (electrode) material to the cathode (metallic part) during the electrical discharge in pulses between the anode and the cathode, discharge which occurs in a gaseous medium. Unlike conventional electro-erosion machining, a pulsed rectifying current with reversed polarity is used at pulse electrical discharge. In this case, the impulse electric discharge process has the air as the gaseous medium. In the deposition technology, the electrode performs a vibratory motion. Due to the polar effect, the predominant transfer of the anode material (electrode) to the cathode (the piece) ensures the formation of the superficial layer with well-defined physic and chemical properties. Upon completion of the discharge, at a very low temperature range, cathode anode removal begins, an action that ends with the electrical circuit break, after which the process is resumed. As a result of the transfer of material and thermal changes from the discharge zone, in the process of superficial discharge of metallic materials with electric sparks, the surface layer of the cathode changes its structure and chemical composition. The characteristics of this layer may vary greatly depending on the electrode material, the composition of the medium between the electrodes, the impulse discharge parameters, and other conditions of the cathode layer formation [23]. Between two sparks, the low quantity of melted metal solidifies, developing a protective layer.

Electrical and working principle of the pulse electric discharge process is shown in **Figure 1**.

The electrical scheme represents a generator, the cathode coupled part, and the electrode as the anode, which is used to form the superficial layers on the part. The surface processing begins with the proximity of the sample electrode and at the critical breaking distance triggering the electrical discharge by impulses, which is often continuous and ends only at the contact of the electrodes. After penetrating the gap between the electrodes, due to the energy accumulated in the C_p capacitor, at the contact surface of the electrodes, strong heated area (local melting and evaporation outbreaks) occurs that causes the electrical erosion of the electrodes (the piece and the electrode itself). The essence deposition using the pulsed electrical discharge method lies in the complexity of physical phenomena which are occurring during the technological process. Discharge parameter regimes (voltage, current, and pulse time)

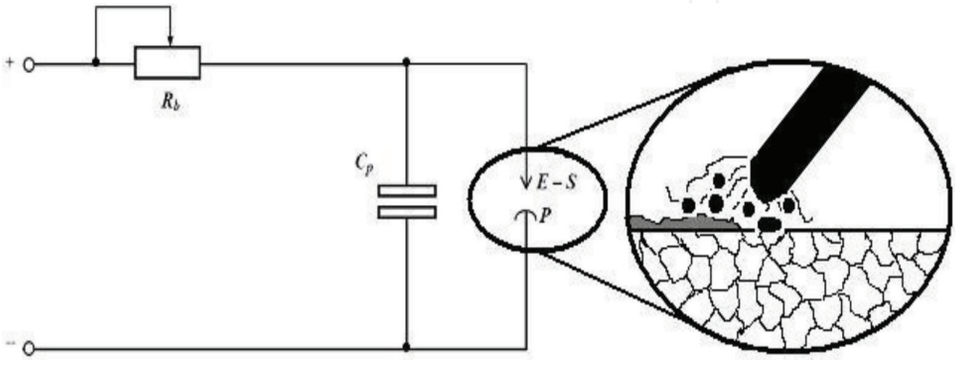

Figure 1. Surface processing using electro-spark deposition method: wiring diagram for the processing device: C_p, condenser; R_b, variable resistance; E-S, electrode connected to the anode; and P, part connected to the cathode.

depend on the physical and chemical properties of the electric and working circuit (device-electrode-base material). In this context, we can say that the parameters depend on the type of electrode deposition, and its melting temperature, the thermal conductivity, chemical reactivity of the anode elements, diffusivity, density, electrical resistance, thermal inertia, flow ability, and parameter temperature dependence.

Among the basic features of the impulse electric discharge method, which also include advantages, can be mentioned: lack of special preparation of the surface to be processed; the deposited layer, due to the high solidification/cooling speed, obtains amorphous-specific properties; the deposited layer does not usually require subsequent finishing; apply easily to the surface of complex parts; the deposition can be done in strictly indicated places; the deposited layer has good adhesion to the support; the possibility of using as electrode both pure metals and their alloys; the possibility of deposition using metal-ceramic materials and hard fusible compounds; lack of heating of the sample in the process of deposition and implicitly of the collateral effects; the effect of pollution is minimal and completely eliminates the use of toxic nonmetallic compounds such as cyanide in the coating process; the necessary equipment is relatively simple, and the technology has costs mainly generated by the quality of the additive materials [23].

Procedure's advantage is that heat density of the piece is minimum maintaining chemical composition and the properties of basic material. The thin layer system hardened through impulse electric discharge method is splitted into: an exterior layer with a strongly modified structure at the surface and an interior layer (diffusion layer) with the properties corresponding to basic material and added material. The hardened layer presents cracks that are advantageous to the lubrication process (during exploitation) by protecting basic material of excessive wear.

An inadequate diffusion is a risk factor for obtaining thin films, their long-term stability, and security in service. This can be solved by applying a heat treatment or thermochemical treatment afterwards. This may cause high electrode consumption due to its elongation and tear, due to the rapid dissipation of heat developed to part contact area, while the heat dissipated in the electrode is made slower, this being due to the large mass difference between the piece and the electrode. This problem can be solved by choosing an optimum working regime using appropriate parameters. Deposited layer characteristics are controlled process parameters: spark energy, discharge voltage, spark duration, inductance, frequency, temperature, number of passes, pressure on the end electrode (filler) on the surface of the base material, linear speed horizontal electrode, etc. The difficulty of the problem, in some cases, to the incompatibility between the filler material is characterized by special properties and support.

For this reason, there is a need for multiple layers: the first layer deposited actually providing the support anchoring surface layer.

2.1. Mass transfer

The mass transfer intensity and coating parameters can vary depending on the electrode material nature and basic material nature. Energetic transfer is depending on the physical and chemical characteristics (specific heat, density conductivity, and thermal transfer coefficient),

on the atomic number, and on the value of the elements that are in the cathode, anode, and work environment composition. The electro-spark deposition can be viewed evolutionarily, over time, by the steps required to form the layer, that is, the proximity of the electrodes, the penetration of the gaseous zone between the electrode and the base material, and also the creation of a thermal flux that has the effect of melting the areas limiting the flow to both the cathode and the anode; creation of a plasma area surrounding the energy and mass transfer field, an area that favors chemical activities, due to the formation of strong reactivity ions [24]. But, the same deposition can also be seen in terms of evolution in space by studying the structure of the areas that make up the deposition system. The deposition areas can be divided according to their position and role in the operation, as follows: anode electrode area (area of the filler material); deposition flow area; part deposited material area; and cathodic area of the base material.

Electrode anodic area. Priming arc between the two electrodes has the first effect, a thermal flux that leads to electrode top melting (**Figure 2a**).

Because of the temperature parabolic variations, the electrode material will melt, so the top of the electrode will take an interior shape like the thermal field. During coating, the initial thermal flux separates, and warm small areas are developed inside the cone. Inside the cone appears small bumps because small warm areas are migrating inside, and the material melting from inside is done depending on local thermal peaks. Tungsten electrode peak pictures show that the cone peak coating is deeper (**Figure 2b**). Electro-erosion energetic flux is creating a small top cone, with high differentiated and with a visible and deep crater. Crater side surface is soft, less involved in coating and plasmatic cinematic processes of the treatment.

Flux area. It is the area with the higher dynamism, here is forming the electrical, thermal, and plasmatic flux, with active elements development: atoms, ions, and electrons. This is influencing

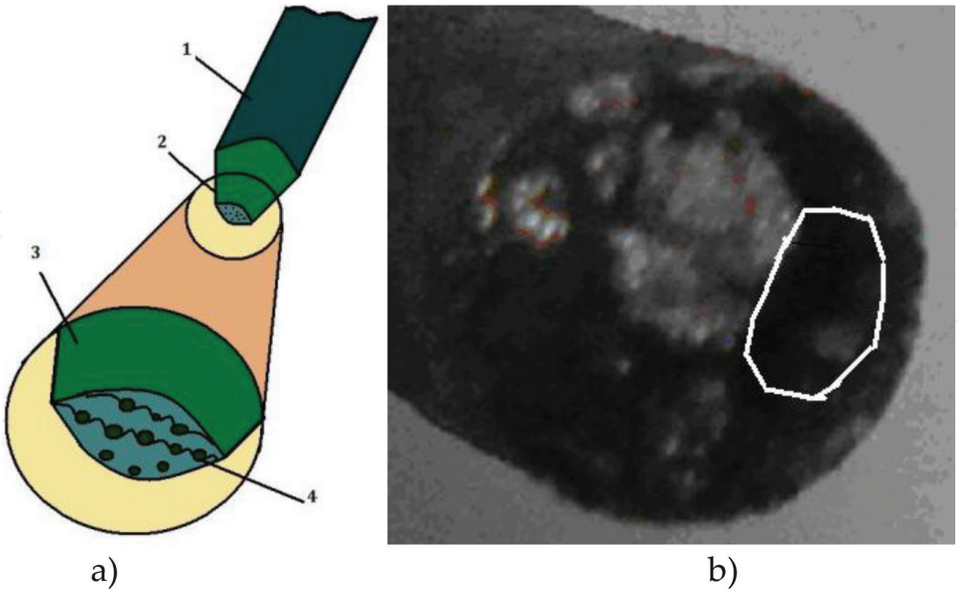

Figure 2. (a) Maximum and minimum of local mass transfer; (1) electrode; (2) attack zone; (3) enlarged attack zone for highlighting the formations at the interior cone base; (4) maximum and minimum local thermal areas developed during mass transfer; (b) tungsten electrode peak used in this experiment.

the character and the quality of the coating. In the flux area (**Figure 3**), are developing, beside high thermal, electrical fields and added material witch strikes with high force. This material is solid (particles) or liquid (drops). Depending on the electrode type, we will have mainly one of the two up-mentioned forms: nickel and titanium have in their flux, mainly, melted material drops, and tungsten, because of high melting temperature created inside the flux, specially extracted particles.

Material deposition area. The area of the deposited material is important because it gives information about the surface characteristics. The amount of melted and deposited material on the surface depends on various parameters, such as: pulse current frequency, gap size, electrode material properties, average intensity, pulse power, etc. Studying the part surface microgeometry modification using the development of the waves on the surface of the liquid metal in the impulse discharge conditions, author Topală (**Figure 4**) writes that the phenomenon is accompanied by the appearance of craters on the surfaces of electrodes [25].

In fact, three types of craters have been recorded, all of them having the shape of a spherical calotte (**Figure 5**): (i) a smooth profile with good flow properties (low relative melting temperature such as Ni and Ti); (ii) a rugged profile, specific for the fragile material electrodes, which

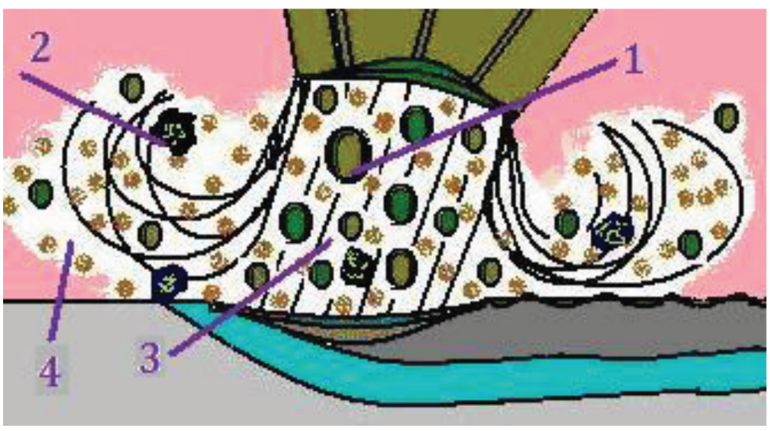

Figure 3. Flux elements; (1) liquid added material (drops); (2) extracted added material (particles); (3) thermal flux—heat jet; and (4) plasma (developed by gases decomposition and nitrogen, oxygen, and carbon active atoms.

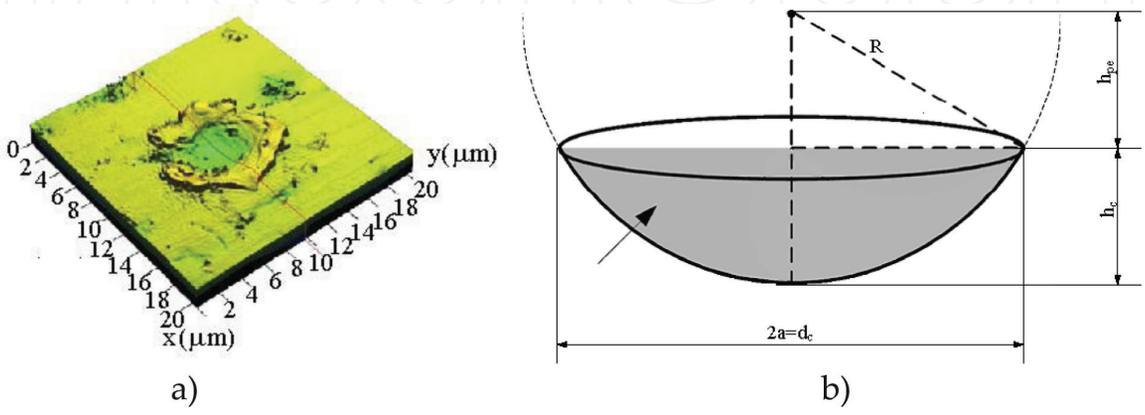

Figure 4. (a) General view of a deposition erosion crater; (b) the spherical calotte is an idealized form of the crater.

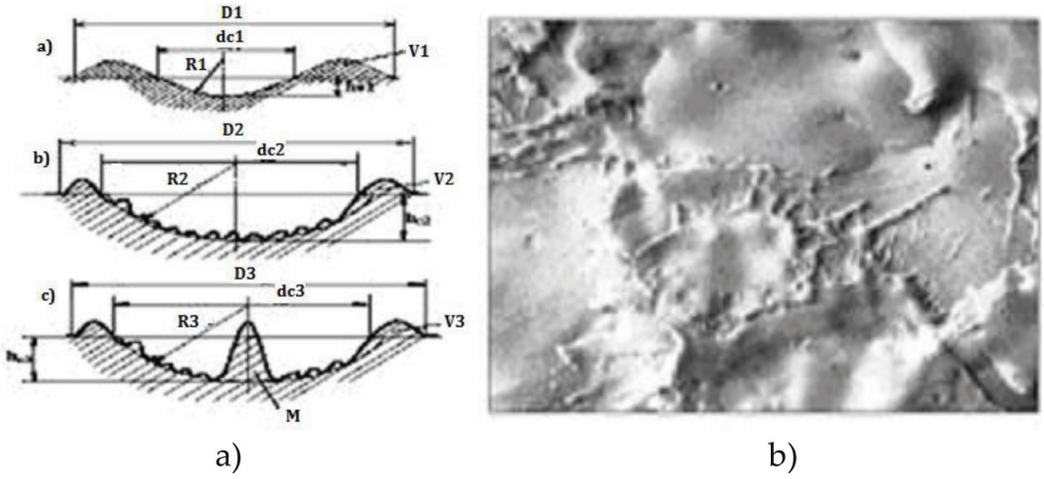

Figure 5. (a) Types of craters obtained by dimensional processing by electroerosion (D_1, D_2, and D_3—the diameter of the craters together with the wave; d_{c1}, d_{c2}, and d_{c3}—the diameters of three types of craters; h_{c1}, h_{c2}, and h_{c3}—The depth of the craters; M—meniscus; and V—wave); (b) the waveform of the deposition surface.

break out during deposition and do not melt easily (due to very high melting temperature, for example, tungsten); and (iii) a middle meniscus, characteristic for materials that solidify at a high rate (high melting temperature, when the "drop" touches the cold part, solidification begins).

The forces that compete to create surface geometry are the ion beam pressure force and the metal vapor reaction force, due to the static pressure of the metal vapors in the crates. It has been noticed that the height of the meniscus depends on the following factors: discharge energy, discharge time, electrode material, and application of the electric field to the gap.

Base material area. This area is important to the necessary consistency with the addition material, so that the small bonding area that ensures the adhesion of the layer is as strong as possible.

2.2. Surface morphology

The hardening of the surface of a piece by the ESD method requires knowledge of the properties of both the basic material (physical and chemical properties) and the deposition material. When heterogeneous multilayer layers are depositing, the base layer must be metallurgically compatible with the adduct and have good adhesion properties and near by physical properties (coefficient of expansion, conductivity, diffusivity, electrical resistance, melting point, and vaporization). The exterior layers must have the characteristics required to operate the part (wear resistance, dynamic shock, corrosion resistance, abrasion resistance, hardness, etc.). In the case of an intermediate layer, the deposited layer and the surface layer must be connected.

Tests were made with the Elitron 22A type machine (**Figure 6**). The device parameters listed in the machine's technical manual are: the power consumed (kVA)—0.5; productivities (cm^2/min)—4; working voltage (V)—220; working regimes (r), amplitude of vibration (A)—(A1 = 0.04 mm, A2 = 0.06 mm, A3 = 0.08 mm, A4 = 0.1 mm, A5 = 0.12 mm, A6 = 0.14 mm, A7 = 0.16 mm, A8 = 0.18 mm, and A9 = 0.2 mm); mass (kg)—21 [26]. The Elitron 22A instrument used in the experiments has nine amplitude and six work modes.

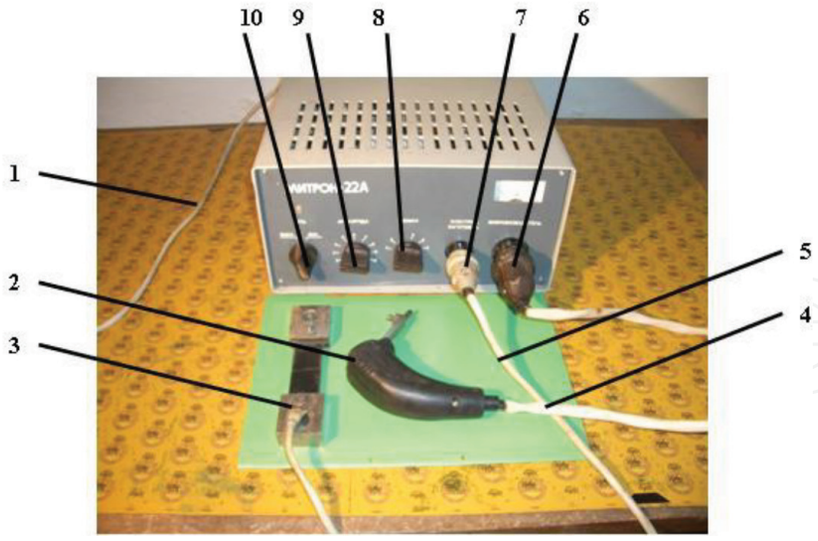

Figure 6. Components of the Elitron 22A pulse electric pulse deposition device: (1) power supply cord; (2) electrode support; (3) piece support; (4) electrode support cable; (5) piece support cable; (6) and (7) connecting sockets; (8) adjustment knob (intensity); (9) vibration amplitude adjustment knob; and (10) stop-start button.

As a base material for the coating, ferritic-pearlitic cast iron was used, which chemical composition is presented in **Table 1**. The chemical composition determined by means of Foundry Master spectrometer.

Justifying the choice of the base material is given by the advantages of choosing this material in textile industry machines and installations (cams, friction skates, and gears in looms). Gray cast iron is a material with a good thermal shock resistance and does not require lubrication. Expanding and contraction coefficients are low and have the property to absorb easily apparent tensions during work by means that graphite from the matrix is creating discontinuities that can absorb vibrations and shock exposure.

Electrodes used for deposition are Ti, TiC, W, and WC. The surfaces of the deposition drops were analyzed by means of electron scanning microscope (SEM).

2.3. Analysis of deposition drops

In the pulsed electric discharge deposition process, in addition to particular importance for the mass, transfer workflow parameters and physicochemical characteristics of the whole area, a great contribution to the achievement of appropriate structures is the type of deposition, and in particular adhesion and microalloying for the drop. As long as the connected metal layers are obtained using this technology, the coating properties are dependent by the chemical reactions at the interface. Since a coating obtained by depositing consists of multiple single drops,

Element	C	Si	Mn	P	Cr	Ni	Cu
Percentage, %	3.97	2.87	0.25	0.06	0.28	0.12	0.17

Table 1. Chemical composition of base material.

formed in a dependent rotary movement order of the electrode is important to study the deposition "drops" generation and also the characteristics for the uni-impulse drops. At the same time, the interface chemical reactions lead to the formation of varied compounds, also influencing the coating properties. The drop represents the part exterior shape after the treatment, because the layer is formed by a lot of drops, some of them remelted by the subsequent crossing. The flattening of the "drops" sputtered on the substrate is one of the most important processes occurring in coatings using electric arc. The layer structure will determine the coating structure and therefore, adhesion and coating properties. Therefore, attention was paid to the study of "drops" by experimental observations.

Analysis of the "droplet" shape using a titanium electrode. It is noticed that the Ti electrode does not only achieve a smooth deposition of the "droplet," but also the process is much more dynamic, the deposition takes place at a certain speed, and the strike impulse creates micro-depression surface, which subsequently, upon the fall of a new "droplet", leads to a microalloying with the subsequent in depth layer (it is at most 20 μm) (**Figure 7**).

The map of the surface elements of the titanium shell (Ti) on the ferrite-perlite substrate is shown in **Figure 8**.

Uniform distribution of the elements can be observed, indicating the complete alloying process between the base and the substrate. The Ti was distributed in the melting zone on the cast iron substrate and by diffusion in area interface. New phases have been formed in the coating layer due to the chemical reaction during the deposition process. Note the titanium distribution in **Figure 8b**.

Thus, due to the high temperature conditions, the following reaction takes place: Ti + C = TiC. The "drop" striking energy on the metal surface is added to the thermal energy and plasma energy that is formed during the deposition. Thus, optimum conditions are created for the formation of highly intermetallic compounds or chemical compounds. Another particular aspect is that Ti compact droplets are distributed at the edge of the droplet rather than the center, this being possible due to the splashing dynamics. An advantage of the

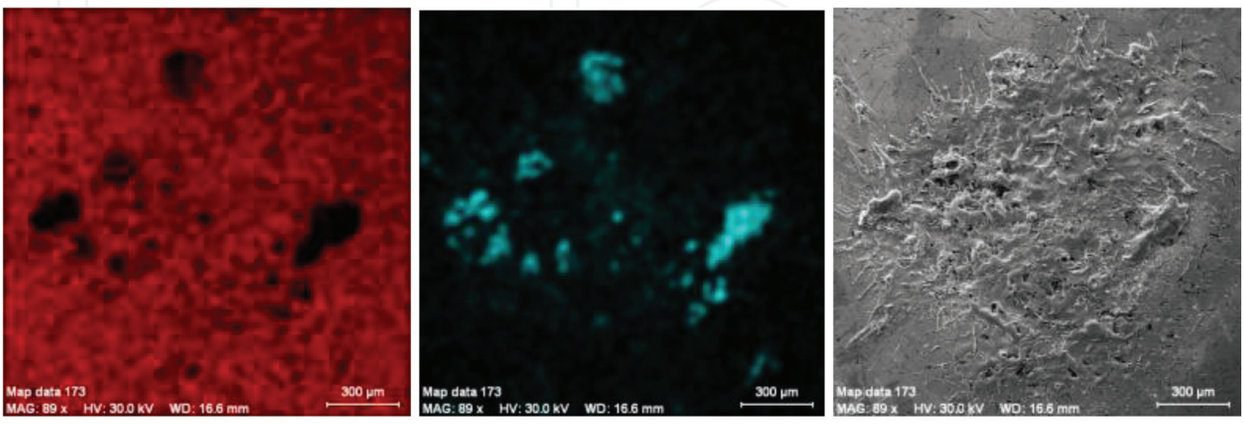

Figure 7. Distribution of Fe and Ti elements; (a) SE_Fe; (b) SE_Ti; and (c) the "drop" by Ti, SE image giving information about surface relief.

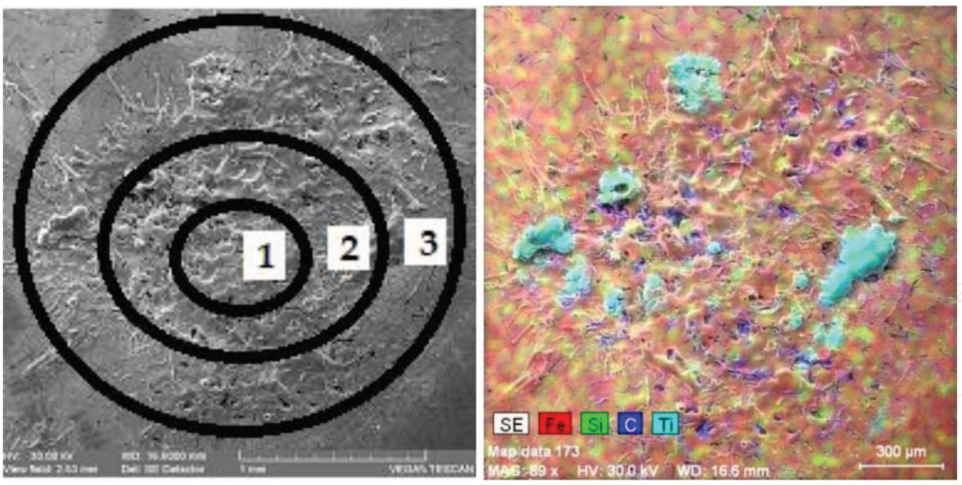

Figure 8. (a) Area distribution of the drop; (b) elemental distribution of the "drop."

melting and solidification dynamics specific to Ti is that there are no large and visible cracks, and the layer is relatively compact.

A disadvantage of the dynamics of the phenomenon is that the roughness of the piece is quite high. Studying the BSE (Back Scattered Electrons) image shows the phase difference by the appearance of dark areas and bright areas, when the surface of the base material contains ferrite grains (light color) with darker vermicular areas (carbon), areas found in higher quantity in the center of the "droplet" (carbon forms titanium chemical compound due to chemical activity of carbon in the plasma). The black areas are made up of Ti droplets. The "droplet" area can be divided into three regions characterized by both the variation of the deposition form and the variation of the deposition element content.

The first region (**Figure 8a**) represents the center of the "droplet" that received the highest energy impulse in the deposition motion, where the temperature was the maximum, and a melting of the substrate took place. In this area, we do not actually encounter Ti in the form of a microdrop, but just accidentally by slashing. In this area, chemical compounds obtained through the reactions between Ti and the substrate elements predominate, facilitated by the energy released in the area.

The second region represents the immediate vicinity area, in the form of an annular shape, and which is a transition zone to the edges of the "droplet". In this area, Ti is found in the form of a compact micromelt, as well as microalloying compounds due to the dynamics of the melting bath and migrating from the center to the outside.

In the third zone, which is the periphery of the "droplet," melted and solidified splashes of Ti are predominant; also drops from the melted substrate pulled away the formation site due to the splashing motion. Also, due to the splashing, bumps are formed by microelevation formation right on the edge of the "drop," while in the center, there are flattened areas with a certain concavity.

The spreading zone is quite large because Ti and its chemical compounds melt at relatively low temperatures and are in a liquid form, a relatively long time (order of seconds). Due to the

fluidity of the drop elements and the fact that the expansion coefficient of the substrate and the drop is almost the same, no visible cracks appear, **Figure 9**.

The outside droplet pores found, the third scattering zone, are derived from the presence of chemically absorbed gases at the surface of the part, or gases from the metal bath reaction.

2.4. Titanium deposition on a cast iron layer

From micrographs made by scanning electron microscope shall be observed that Ti deposition on cast iron electrode creates a relatively compact layer with limited bumps and obvious cracks. Titanium shall be uniformly deposited both highlighted in **Table 2** by its high percentage and the EDX analysis (**Figure 10**), when is observed the distribution of the titanium deposition on almost the entire surface.

Titanium coatings are compact, as the atomic number of Ti (22) is much closer to that of Fe (26), which means that their atomic radius difference is very small. This makes it easy to transfer the titanium on the substrate. The outer layer of iron underwent a partial melting allowing for titanium microalloying, but mainly the layer is thin, micro interrupted.

Alloying titanium base material is achieved in a smaller extent because of high melting titanium temperature (1800°C) making titanium to quickly solidify once reached the surface. Thus, it explains the presence of areas with excess deposited material (compact undissolved titanium areas into "drop" metal bath and stuck to the surface). At Ti deposition on gray cast

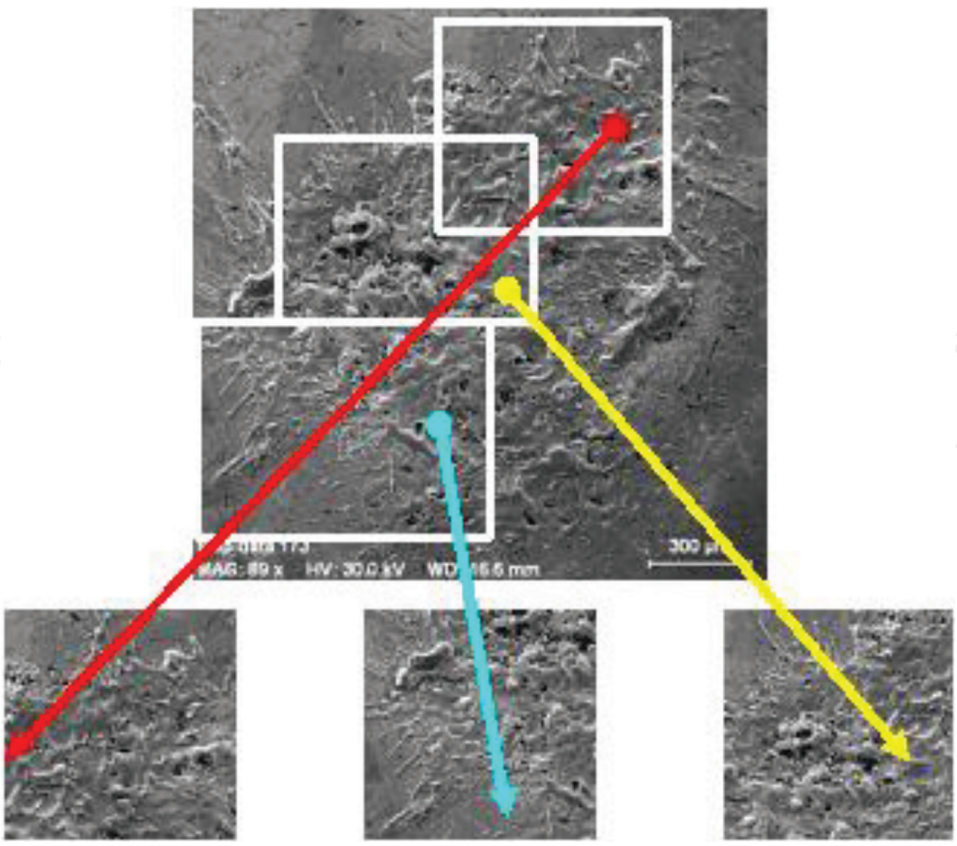

Figure 9. Enlarged areas in the SEM image are for highlighting the extent of spreading of the melted area.

Element	Volume percent, (%)	Atomic percent, (%)
Titanium	76.56	77.64
Iron	22.36	19.44
Carbon	0.46	1.89
Silicon	0.44	0.76
Phosphorus	0.16	0.27

Table 2. Chemical composition for Ti deposition on cast iron.

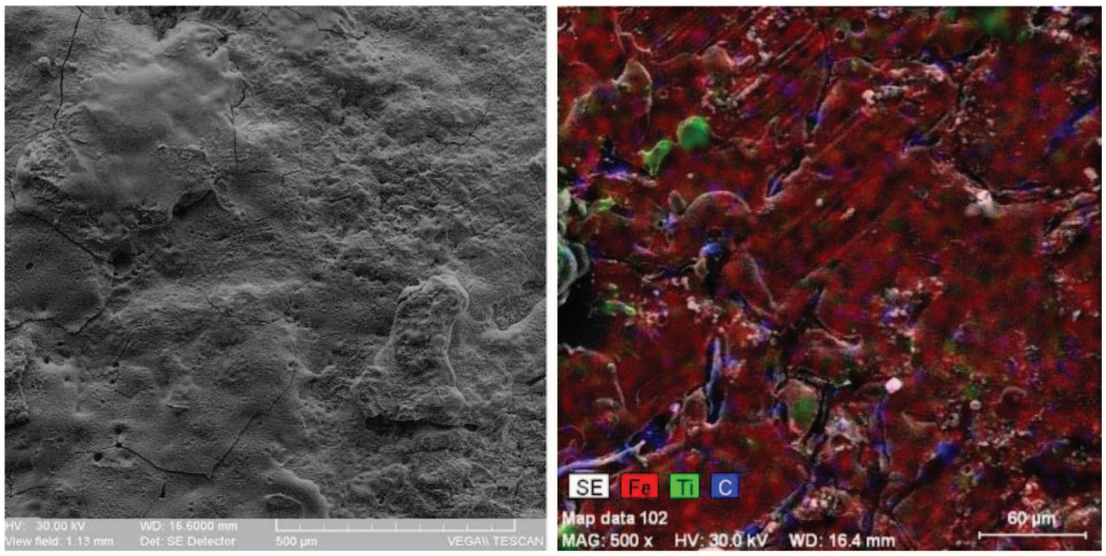

Figure 10. (a) SEM microstructure; single layer Ti deposition on cast iron, SE, 500 μm scale; (b) elements distribution by EDX analysis, 60 μm.

iron, the graphite slides do not melt and dissolve in the microzones of the deposition drops. Due to this, the lamellas absorb the heat and release it gradually, keeping the surface warm for a long time, resulting in a more complete distribution of Ti deposited on the surface.

2.5. One-way deposition and two-way deposition using Ti electrode

In one-way deposition, the deposits with Ti electrode (**Figure 11a**) are compact, due to the atomic number of Ti which is closer to Fe meaning that the difference of atomic radius is very small. This makes titanium transfer easily from interface to substrate. The exterior layer of the ferritic-pearlitic iron stands a partial melting, which made possible titanium micro alloying.

It achieved a thin layer with discontinuous micro zones, without material withdrawals. Titanium has good coating qualities when base material is ferritic-pearlitic iron. The images and the chemical composition of the layer are achieved by means of electronic scanning microscope.

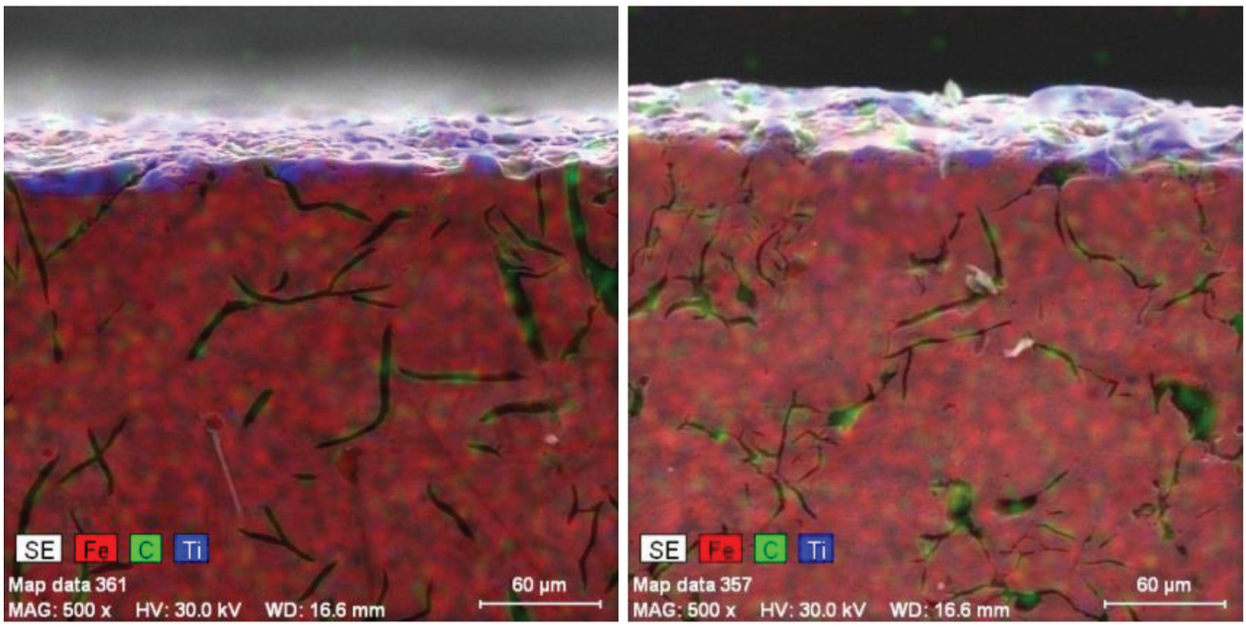

Figure 11. (a) Distribution of Fe, C, and Ti elements for one-way deposition, 500X; (b) distribution of Fe, C, and Ti elements for two-way deposition, 500X.

In **Figure 11b**, notices zones with microcracks due to the increase of the superficial layer and to the fact substrate is colder than in one-way deposition, so that the cracks are less pronounced. It is also possible that the cracks are only in the first layer and do not get into the second layer.

In **Table 3**, it is given the chemical composition of the deposit layer with Ti electrode, one-way deposition. The chemical composition of the deposit layer with Ti electrode, two-way deposition, presents in **Table 4**. Element distribution presents common repartition areas of Fe, C, and Ti, indicating the presence of intermetallic compounds within alloying bath. Microzones with cementite can be seen in the microstructure due to the energy application of the thermal flow and due to the powerful temperature gradient at cooling (the exterior layer cools down quickly). Cooling takes place due to air contact and to the small thickness of the layer (some tens of microns).

The layer thickness, (**Figure 12a**), Ti deposited (one-way deposition) varies between 24.75 and 30.63 μm, indicating a good uniformity of deposition with very small deviations from the flatness of the surface and a low roughness.

When analyzing the layer thickness (two layers of titanium, **Figure 12b**), it is observed, by examining electron micrographs, that the outer layer of Ti two-way deposition creates a surface as smooth as depositing a Ti layer. The thickness of Ti layer by deposition of two passes is uniform and varies between 36.52 and 47.72 μm.

Blanking, titanium deposition (**Figure 13a**) is a thin layer with good adhesion because the rupture is smooth, without exfoliation. The breakage of the layer is similar to a fragile crack due to the higher hardness of the coating over the base material. Analyzing the micrographs

Element	Iron	Carbon	Titanium	Silicon
Percentage, %	88.32	7.25	2.41	1.99

Table 3. Chemical composition of one-way deposition of Ti layer.

Element	Iron	Carbon	Titanium	Silicon
Percentage, %	58.82	35.59	3.58	1.99

Table 4. Chemical composition of two-way Ti layer.

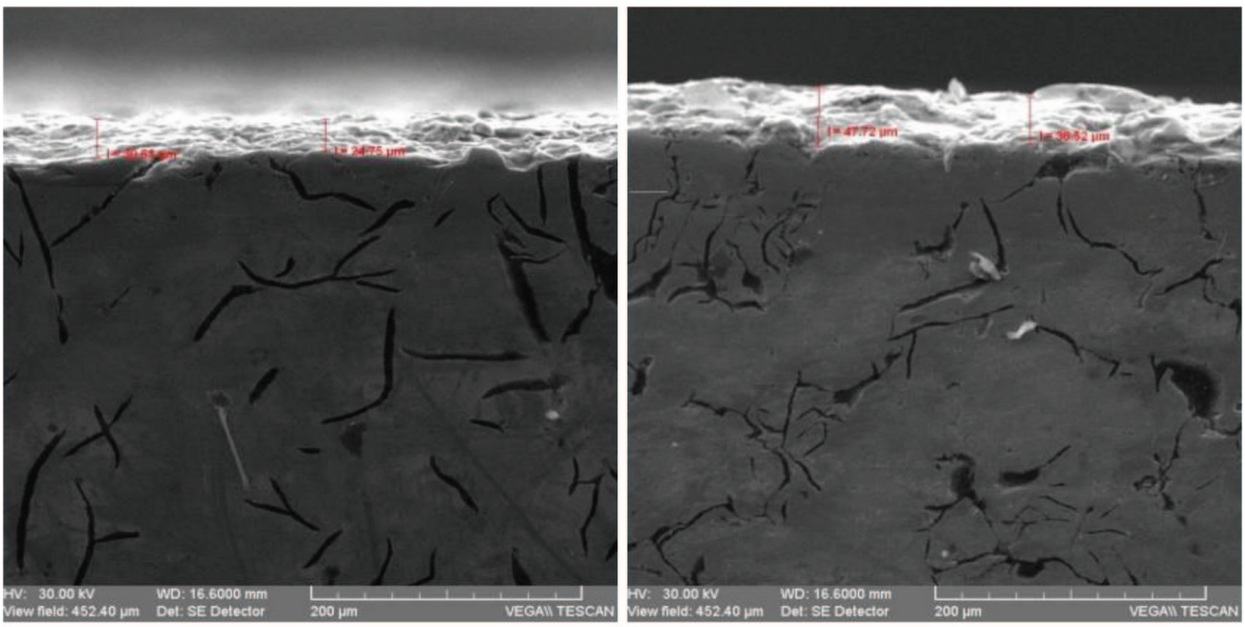

a) b)

Figure 12. (a) Thickness value for depositing one-way deposition Ti layer; (b) thickness for deposition of Ti two-way layer.

obtained in the electronic scanning microscope for two-layer titanium casting test specimen (**Figure 13b**), the deposition and compactness of the layer were observed.

The deposition of titanium in the quartz has a characteristic form of breakage due to the high hardness of the deposited area.

2.6. Ti/W/TiC deposition analysis

Heterogeneous triple deposition begins by depositing a titanium layer on the surface of the base because it has good adhesion, depositing relatively compact, no gaps, no strong oxide layers, and no massive roughing on the surface of the sample. Titanium has the property of being a good support for mechanical and thermal shocks. The second layer is a tungsten electrode, which is a hard material with a very high melting temperature that creates deposition craters and areas of material gaps but improves the hardness of the deposited layer. Titanium

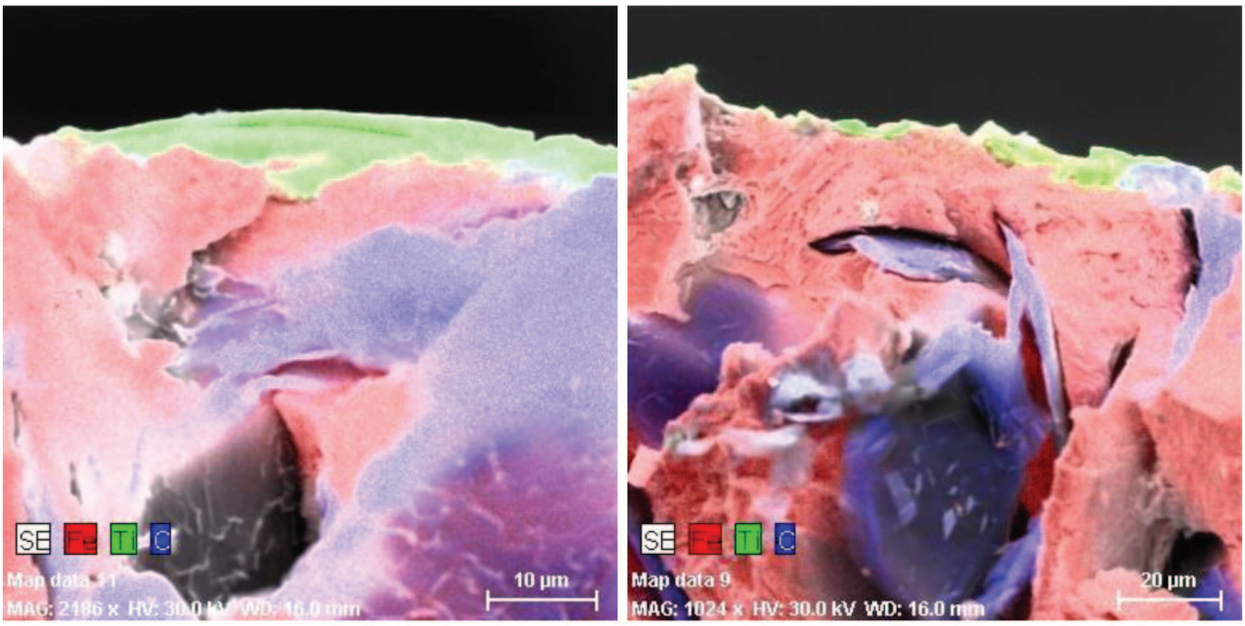

Figure 13. Distribution of elements in the crack; (a) simple Ti deposition: Ti, Fe, and C; (b) deposition Ti double layer: Ti, Fe, and C.

carbide alleviates the defects introduced by tungsten by smoothing out surface roughness and covering areas with crackers and squeezing of the material.

Studying the EDX analysis is observed in the presence of a 32.42% of tungsten and just 13% titanium (**Table 5**) [27].

A layer thickness analysis was made. It is observed that the triple layer has a relatively even thickness, and the variation of the thickness is proportional with the roughness of the surface. The thickness of the layer varies between 172 and 119 μm (**Figure 14**), meaning that is a relatively thick layer. The surface layer can be grinded, after that also the thickness is relatively high [27].

In the fracture, the combination of triple base deposition material presents as a fragile rupture due to the high hardness of the deposited layer. It is noticed that the deposition has not separated, which shows a microalloy with the large diffusion area that creates the adhesion between the deposited layer and the base material.

This ensures the deposited layer a hybrid structure with amorphous feature, containing a layer with deposition elements dissolved in high concentration in basic matrix on a smaller distance than 100 μm [27].

2.7. XPS analysis for the sample with WC/TiC/W deposition

The analyses were done on multi-layer depositions, namely, tungsten carbide—as the first interface and titanium carbide—as the second interface and tungsten exterior layer (WC/TiC/W), being made with PHI 5000 Versa Probe-XPS X-ray photoelectron spectrometer. The determination of energetic maximum (energetic peaks) gives indications on the chemical compounds

Element	Iron	Carbon	Tungsten	Titanium
Percentage, %	49.82	4.67	32.41	13.07

Table 5. Chemical composition of the Ti/W/TiC layer.

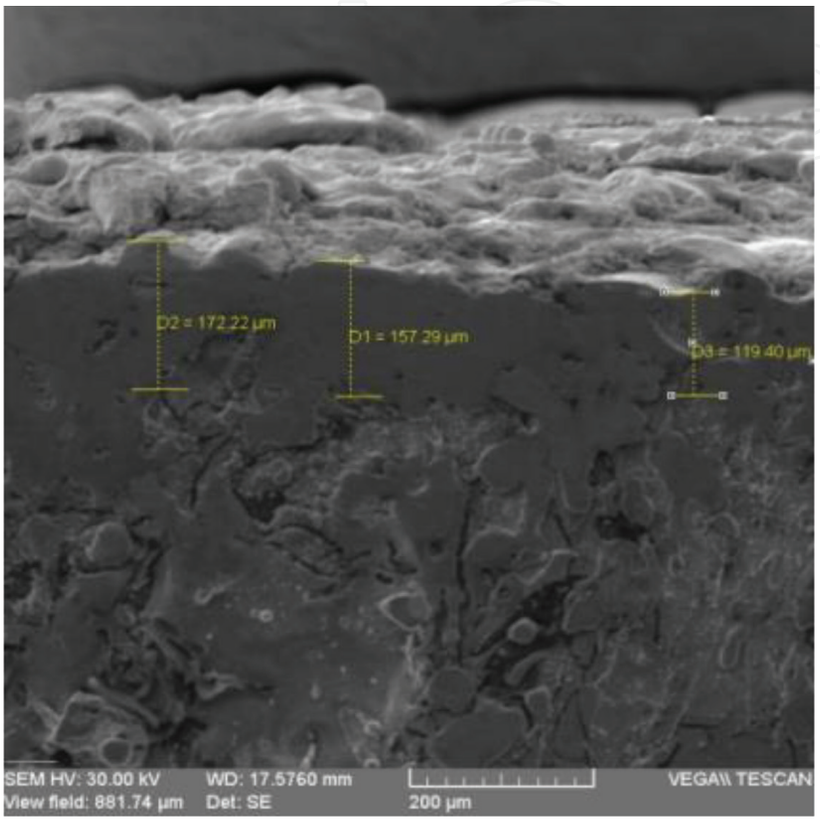

Figure 14. Deposition layer thickness Ti/W/TiC; 200 μm.

of that element in the energy area corresponding to the photoelectronic spectrum of kinetic energy. For the sample with WC/TiC/W deposition are presented two graphs generated at different radiation times, the first at 16.01 minutes (**Figure 15a**) and the second at 32.01 minutes (**Figure 15b**). Exposure time was increased to remove the effects of contamination because elements such as Si, P, and Ni appear in small percentages, being elements that occur through absorption on surface during deposition or later on. In general, graphs notice the presence of the chemical elements on the surface as well as the orbitals of each element such as C1s—28.6%, Fe2p3—22.4%, Ti2p—8.1%, and W4f—6.5% and from the atmosphere O1s—30.6% and N1s—3.1% [28].

The graph with local maxima is presented showing chemical elements and bonds in the energetic range of 0–1200 eV. For each chemical element, the energetic bonds were studied such as the chemical compounds appeared in the layer and so enlarged areas in the energetic scale realized.

- for C1s between 274 and 296 eV. In the area maxima peaks discovered that correspond to the following compounds CO_2, CO_3, TiCN, TiC, WC. Local energetic maximum areas are listed in **Table 6** for each chemical compound in whose composition carbon enters.

http://dx.doi.org/10.5772/intechopen.79450

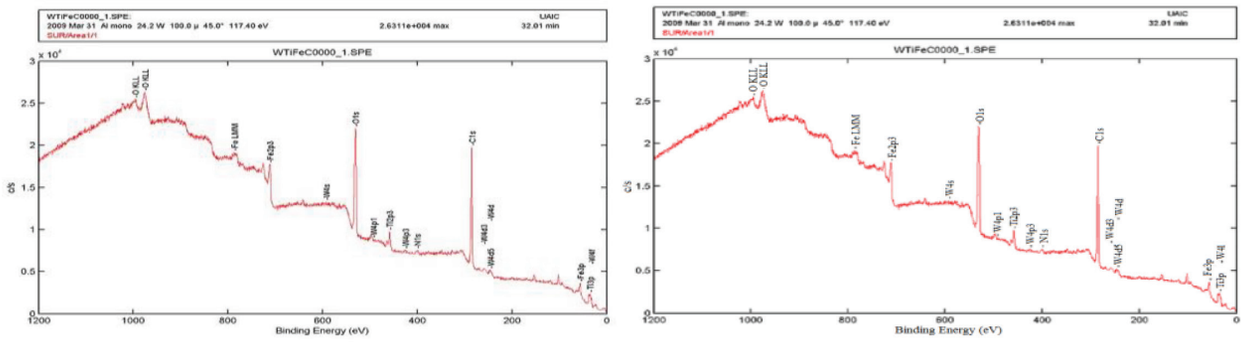

Figure 15. General graph obtained at radiation time for WC/TiC/W deposition at duration of: (a) 16.01 minutes; (b) 32.01 minutes.

Chemical compound	CO_2	CO_3	TiCN	C	TiC	WC
Energetic maximum (eV)	291.6	290.2	288.7	285.1	281.2	281.1

Table 6. Local energetic maximum areas for each compound.

- for O1s with the energetic band between 522 and 544 eV local extremes decompose appropriate to the following oxides Fe_2O_4, TiO_2, TiNO, WO_3, Ti_2O_4. Local energetic maximum areas are listed in **Table 7** for each chemical compound in whose composition oxygen enters.
- for Fe2p3, **Table 8**, with the energetic band between 700 and 740 eV, it notices local maxima in the energetic range of the following chemical compounds Fe_2O_3, FeOOH, $FeWO_4$, FeO, Fe_3O_4, and Fe_3C.
- for Ti2p3, **Table 9**, with the energetic band between 450 and 475 eV, emphasizes the local maxima from this energetic range corresponding to the following chemical compounds TiO_2, TiC, TiN, Ti_2O_3, and TiC, **Figure 16**.
- for W4f, **Table 10**, with the energetic band between 25 and 45 eV, emphasizes the local maxima from this energetic range corresponding to the following chemical compounds $Fe_2(WO_4)_3$, WO_2, WO_3, and W.

The presence of massive amounts of oxides is due to the deposition in air without a protection layer but only with the protection of the plasmatic atmosphere between cathode and. Oxygen

Chemical compound	Fe_2O_4	TiO_2	TiNO	WO_3	Ti_2O_4
Energetic maximum (eV)	536.7	529.4	531.1	531.1	531.1

Table 7. Local energetic maximum areas for each compound.

Chemical compound	Fe_2O_3	FeOOH	$FeWO_4$	FeO	Fe_3C
Energetic maximum (eV)	715.7	710.7	711.5	711.1	707.1

Table 8. Local energetic maximum areas for each compound.

Chemical compound	TiO_2	TiC	TiN	Ti_2O_3	TiC
Energetic maximum (eV)	464.9; 458.4	454.8; 460.1	454.8; 463	455.8	455.1

Table 9. Local energetic maximum areas for each compound.

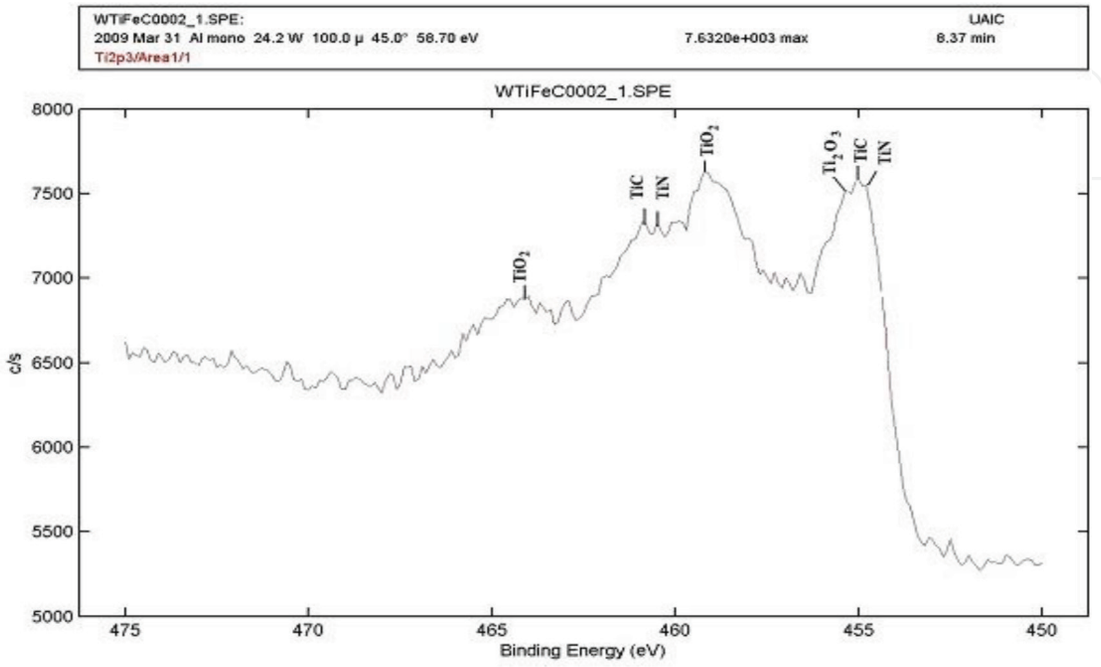

Figure 16. XPS analysis for Ti2p3 at the ferrite pearlite iron sample covered with WC/TiC/W triple layer.

Chemical compound	$Fe_2(WO_4)_3$	WO_2	WO_3	W
Energetic maximum (eV)	36.4	34.1	34.1	31.8

Table 10. Local energetic maximum areas for each compound.

and active nitrogen are also present in this atmosphere, as demonstrated by the presence of the compounds such as TiCN, WO_2, WO_3, TiO_2, FeO, Fe_2O_3, Fe_3O_4, FeOOH (rust), TiNO, and Ti_2O_3.

2.8. Thermal conductivity analysis for deposit layers

Thermal conductivity analysis for deposit layers with vibrating electrode method accomplished with Mathis TCI apparatus [29].

In case of thin layer deposition, some peculiar phenomena appear and conductivity varies in terms of deposit layer nature, deposit technology, number of deposit layer, and layer compactness. Between the properties that influence thermal conductivity, we mention besides porosity degree of the layer, deposition irregularity (drops appearance, material discontinuities, and high roughness), hardness (inverse proportional to conductivity), and thickness of the deposit layers, too, **Table 11**.

Material	Value of thermal conductivity, k (W/m K)
Base material	24.41
One-way Ti layer	18.34
Two-way Ti layer	10.59
One-way TiC layer	20.67
Two-way TiC layer	16.70

Table 11. Values of thermal conductivity for base material and all kinds of deposition.

The values for thermal conductivities, **Figure 17**, are very different, being much smaller than base material value. Thin layer depositions with Ti and TiC electrodes on base of ferritic-pearlitic gray iron create thermal barriers in the deposited piece. Thermal barrier has a positive effect because during functioning, at reduced heating, small dilatations appear, so thermal stresses with high values are not introduced in the piece and decrease the danger of deformation appearance or even thermal fatigue, which leads to piece cracking. One can meet an emphasized blockage of thermal transfer at one-way heterogeneous depositions, due to atomic lattice modification, in terms of addition materials and deposition sequence.

2.9. Hardness analysis of the deposit layers

In choosing the method for microhardness determining, it must be taken into consideration layer's structure and properties. For Ti and TiC, W and WC electrodes were made microhardness measurements with Vickers method. PMT3 microhardness machine was used. Pressing weight of the diamond indenter was 50 g (HV50), **Table 12**. The samples were grinded and polished after deposition, and microhardness measurements accomplished due to the small thickness of the deposit layer.

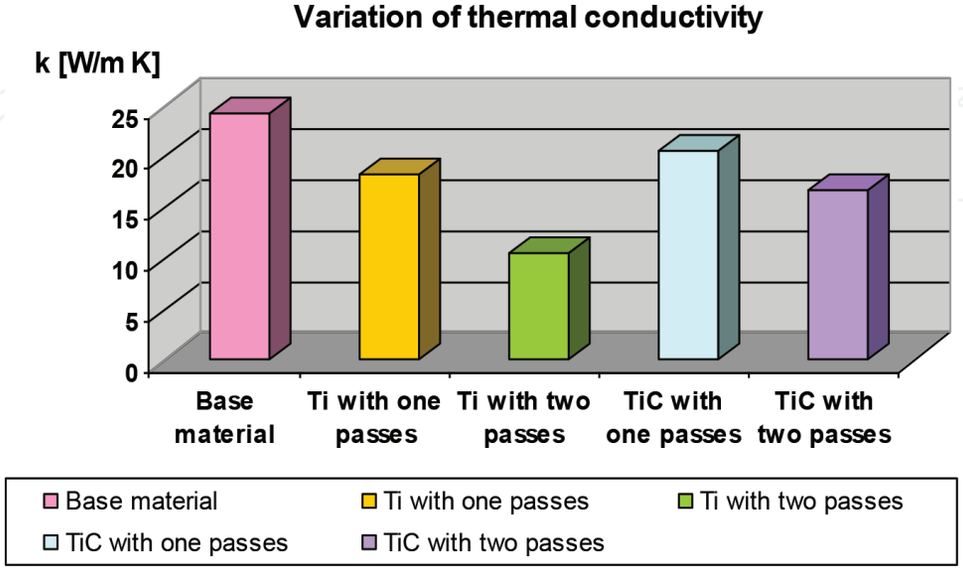

Figure 17. Graphic of thermal conductivity variation for thin layer deposition with vibrating electrode method.

Base material	400.00
One-way Ti layer	729.96
Two-way Ti layer	786.53
One-way TiC layer	773.20
Two-way TiC layer	816.32
One-way W layer	754.42
Two-way W layer	818.32
One-way WC layer	976.56
Two-way WC layer	821.54

Table 12. Values of microhardness measurements for deposit layers, HV50.

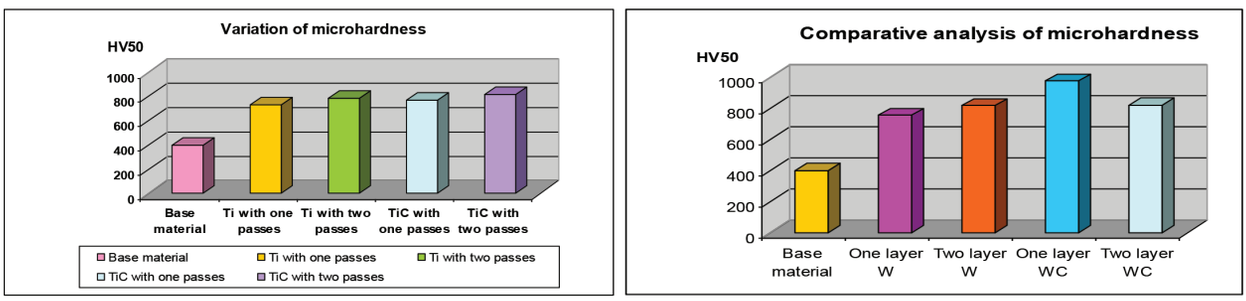

a) b)

Figure 18. (a) Comparison analysis regarding microhardness for simple and double coatings using Ti and TiC electrodes; (b) comparison analysis regarding microhardness for simple and double coatings using W and WC electrodes.

The indenter acted on sample section, and not on deposit surface, so that values represent only the hardness of the layer and not of the base material. Analyzing **Figure 18a** notices that the microhardness values of the thin layer achieved by vibrating electrode method are close to all types of deposition, but double as value against the value of the base material (ferritic-pearlitic iron). Analyzing **Figure 18b** notices that the microhardness values of the thin layer achieved by vibrating electrode method are close to all types of deposition, but double as value against the value of the base material (ferritic-pearlitic iron).

3. Conclusions

The study of ESD deposition is useful for the wide range of application elements used and the multitude of aspects addressed (micronutrition measured in the layer section, internal stresses, roughness, conductivity, EDX analysis, and XPS analysis for the detection of types of chemical compounds obtained in postdeposition and mass and energy transfer analysis, etc.).

The chemical analysis of deposited strands using photoelectron spectroscopy reveals the presence of complex chemical compounds such as carbides, nitrides, oxides (W3C0, 375, Ti_2C,

TiN, TiNO, and TiCN) in the layer, which explains the mechanical properties of the surface layer (microhardness).

The solution is multiple layers, with the advantage to obtain a greater diffusion, which leads to a better anchoring for the layer, with no effect on the surface quality.

The surface quality resulting from deposition using the pulse electric discharge method is dependent on the quality and chemical composition of the electrode. We used Ti, TiC, W, and WC electrodes, and we can conclude that Ti and TiC create much smoother surfaces than those obtained with W and WC electrodes. Titanium has a good adhesion to the surface of ferrite-perlite iron, creating compact layers, with no major bumps and few microholes. Tungsten "burns" the contact surface due to the high temperatures generated in the electric arc, does not deposit itself on the piece, but only makes superficial quenches. Titanium carbon and tungsten carbide have affinity to the ferrite base matrix creating homogeneous layers but with pronounced cracks due to the coefficient of expansion different from the base material.

It notices the influence of the chemical elements from working atmosphere (oxygen and nitrogen), leading to compound formations in the superficial layer. Thus, it notices the presence of Fe, Ti, and W oxides as well as complex nitrides and carbides.

Thermal conductivity of coated surfaces is considerable inferior from the base material. In these conditions, we can conclude that each coating is forming a thermal shield, fact that can be exploited in technical field, in case of using cast-iron for elements that must resist to thermal shocks: heating systems and burning chambers.

From metallurgical aspects point of view, for homogeneous surfaces, we can conclude that tungsten electrodes and tungsten carbide are benefic in increasing the surface hardness.

In order to obtain surfaces with superior qualities, it is possible to combine the method of deposition by impulse discharge with laser treatment or with thermal spraying treatment in order to retrieve the deposited surface in order to obtain more compact layers without cracks and with low roughness.

Author details

Petrică Vizureanu*, Manuela-Cristina Perju, Dragoş-Cristian Achiţei and Carmen Nejneru

*Address all correspondence to: peviz2002@yahoo.com

"Gheorghe Asachi" Technical University Iasi, Romania

References

[1] Wang Y, Ma H, Li X. MATEC Web of Conferences: Interface behavior of tungsten coating on stainless steel by electro spark deposition. 2015;**35**:01006. DOI: 10.1051/matecconf 20153501006

[2] Peterkin S. Electro-spark deposition machine design, physical controls and parameter effects [thesis]. Waterloo, Ontario, Canada; 2016

[3] Radek N, Sladek A. Journal of the Balkan Tribological Association: Properties of electro-spark coatings deposited on the steel substrate using the tungsten carbide-ceramic electrodes. 2016;**22**:1354-1362. DOI: WOS:000381330600026

[4] Huang QS, Chen ZG, Wei X, Wang L, Hou ZW, Yang W. China Surface Engineering: Effects of pulse energy on microstructure and properties of Mo2FeB2-based ceramet coatings prepared by electro-spark deposition. 2017;**30**:89-96. DOI: 10.11933/j.issn.1007-9289.20170106002

[5] Ribalko AV, Korkmaz K, Sahin O. Surface and Coating Technology: Intensification of the anodic erosion in electrospark alloying by the employment of pulse group. 2008;**202**:3591-3599. DOI: 10.1016/j.surfcoat.2007.12.037

[6] Ekmekci B. Applied Surface Science: Residual stresses and white layer in electric discharge machining (EDM). 2007;**253**:9234-9240. DOI: 10.1016/j.apsusc.2007.05.078

[7] Cadney S, Goodall G, Kim G, Moran A, Brochu M. Journal of Alloys and Compounds: The transformation of an Albased crystalline electrode material to an amorphous deposit via the electrospark welding process. 2009;**476**:147-151. DOI: 10.1016/j.jallcom.2008.09.017

[8] Cheng Y, Cai W, Li HT, Zheng YF, Zhao LC. Surface and Coating Technology: Surface characteristics and corrosion resistance properties of TiNi shape memory alloy coated with Ta. 2004;**186**:346-352. DOI: 10.1016/j.surfcoat.2004.01.012

[9] Liu DY, Gao W, Li ZW, Zhang HF, Hu ZQ. Materials Letters: Electro-spark deposition of Fe-based amorphous alloy coatings. 2007;**61**:165-167. DOI: 10.1016/j.matlet.2006.04.042

[10] Frangini S, Masci A. Surface and Coating Technology: A study on the effect of a dynamic contact force control for improving electrospark coating properties. 2010;**204**:2613-2623. DOI: 10.1016/j.surfcoat.2010.02.006

[11] Heard DW, Brochu M. Journal of Materials Processing Technology: Development of a nanostructure microstructure in the Al-Ni system using the electrospark deposition process. 2010;**210**:892-898. DOI: 10.1016/j.jmatprotec.2010.02.001

[12] Kambakas K, Tsakiropoulos P. Materials Science and Engineering A: Solidification of high-Cr white cast iron-WC particle reinforced composites. 2005;**413**:538-544. DOI: 10.1016/j.msea.2005.08.215

[13] Luo C, Xiong XA, Dong SJ. Transactions of Nonferrous Metals Society of China: TiB2/Ni coatings on surface of copper alloy electrode prepared by electrospark deposition. 2011;**21**:317-321. DOI: 10.1016/S1003-6326(11)60715-2

[14] Parkansky N, Beilis II, Boxman RL, Goldsmith S, Rosenberg Y. Surface and Coating Technology: Anode mass loss during pulsed air arc deposition. 1998;**108**:253-256. DOI: 10.1016/S0257-8972(98)00652-5

[15] Miller T, Lin JM, Pirolli L, Coquilleau L, Luharuka R, Teplyakov AV. Thin Solid Films: Investigation of thin titanium carbonitride coatings deposited onto stainless steel. 2012;**522**:193-198. DOI: 10.1016/j.tsf.2012.08.012

[16] Miller T, Pirolli L, Deng F, Ni CY, Teplyakov AV. Surface and Coating Technology: Structurally different interfaces between electrosparkdeposited titanium carbonitride and tungsten carbide films on steel. 2014;**258**:814-821. DOI: 10.1016/j.surfcoat.2014.07.076

[17] Xie YJ, Wang MC. Surface and Coating Technology: Microstructural morphology of electrospark deposition layer of a high gamma prime superalloy. 2006;**201**:691-698. DOI: 10.1016/j.surfcoat.2005.12.034

[18] Chen Z, Zhou Y. Surface and Coating Technology: Surface modification of resistance welding electrode by electrospark deposited composite coatings: Part I. Coating characterization. 2006;**201**:1503-1510. DOI: 10.1016/j.surfcoat.2006.02.015

[19] Chen Z, Zhou Y. Surface and Coating Technology: Surface modification of resistance welding electrodes by electrospark deposited composite coatings Part II. Metallurgical behavior during welding. 2006;**201**:241-243. DOI: 10.1016/j.surfcoat.2006.04.010

[20] Abboud JH, Benyounis KY, Olabi AG, Hashmi M. Journal of Materials Processing Technology: Laser surface treatments of iron-based substrates for automotive application. 2007;**182**:427-431. DOI: 10.1016/j.jmatprotec.2006.08.026

[21] Perju MC, Tugui CA, Nejneru C, Axinte M, Vizureanu P. ESD morphology deposition with WZr8 electrode on austenitic stainless steel support. In: International Conference on Innovative Research—ICIR Euroinvent; 19-20 MAY 2016; Iasi, Romania: ICIR; 2016. p. 012025

[22] Anisimov E, Khan AK, Ojo OA. Materials Characterization: Analysis of microstructure in electro-spark deposited IN718 superalloy. 2016;**119**:233-240. DOI: 10.1016/j.matchar.2016.07.025

[23] Perju MC, Găluşcă DG, Nejneru C, Agop M. Thin Layers: Impulse Discharge. Iasi, Romania: Ars Longa Publishing House; 2010. p. 339. ISBN 978-973-148-049-7

[24] Vizureanu P, Perju MC, Găluşcă DG, Nejneru C, Agop M. Metalurgia International: Mass transfer for titan and tungsten electrode coating using impulse discharge method. 2010;**12**:59-64

[25] Topala P, Slatineanu L, Dodun O, Coteata M, Pinzaru N. Materials and Manufacturing Processes: Electrospark deposition by using powder materials. 2010;**25**:932-938. DOI: 10.1080/10426910903447238

[26] Elitron 22 Installation. Republic of Moldova, Chisinau: Academy of Sciences; 1992

[27] Nejneru C, Perju MC, Axinte M. Applied Mechanics and Materials: Researches regarding Ti/W/TiC triple layers deposition on the ferritic-pearlitic cast iron support, obtained by electro-spark deposition method. 2013;**371**:363-367

[28] Perju MC, Vizureanu P. Revista de Chimie (Bucharest): Chemical compounds analysis developed on the micro alloying area of coating layers obtained by impulse discharge method. 2014;**65**:694-696. DOI: WOS:000339140400013

[29] Largeanu AE, Nejneru C, Perju MC, Galusca DG. Metalurgia International: Thermal conductivity analysis for metallic systems obtained multiple coating by electro-spark deposition method. 2011;**16**:43-46. DOI: WOS:000289606200010

IntechOpen